Fire Safety Journal 162 (2026) 104711

Contents lists available at ScienceDirect

Fire Safety Journal

journal homepage: www.elsevier.com/locate/firesaf

Fire performance of thin intumescent coatings: Material characterisation and application to mass timber structures

Stavros Spyridakis [a,b,*], Felix Wiesner [a,c], Andrea Lucherini [d], Wenxuan Wu [a], Cristian Maluk [a,e], Anwar Orabi [a]

[a] School of Civil Engineering, The University of Queensland, Brisbane, Australia
[b] Fire Science Group, Halliwell, Brisbane, Australia
[c] Department of Wood Science, The University of British Columbia, Vancouver, Canada
[d] Department for Fire-Safe Sustainable Built Environment (FRISSBE), Slovenian National Building and Civil Engineering Institute (ZAG), Slovenia
[e] DAMA Engineering Consultants, London, United Kingdom

ARTICLE INFO

Keywords:
Mass timber
Thin intumescent coatings
Swelling
Fire testing
Charring
Fire safety

ABSTRACT

This study investigates the thermal behaviour of two opaque and one transparent thin intumescent coating at material level (coating only) and system level (coating applied at real scale on timber), and their effects on timber in fire. Micro-scale tests were conducted to examine the underlying mechanisms of intumescence and degradation for each coating individually, while bench-scale tests demonstrated how these behaviours translate to larger scales. Critical temperature and heat flux thresholds were identified at which the coatings begin to insulate the timber through the formation of the intumescent char layer, as well as those marking degradation of the layer and the reduction of its insulating efficacy. The findings highlight that coating type and thickness, heating conditions and exposure duration influence mass retention, swelling pattern, and the integrity of the intumescent char layer. Overall, the transparent coating exhibited lower durability than the opaque ones. It was also shown that, due to the similar temperature ranges of timber pyrolysis and coating swelling, timber degradation occurs close to the coated surface during the transient swelling process, resulting in a heated region of 15-20 mm with negligible mechanical properties by the end of swelling. Therefore, intumescent coatings provide insulation progressively rather than immediately.

1. Introduction

Mass timber structures are considered a sustainable form of construction that has been steadily gaining popularity in the building industry due to its lower carbon footprint relative to concrete and steel [1–4]. However, one of the most severe challenges to the safe adoption of mass timber is its flaming combustion and thus its participation in the fire as fuel, altering the fire dynamics by impacting each phase of the fire. Large-scale fire testing has shown that mass timber compartments undergo rapid fire growth [5,6], generally experience higher temperatures than non-combustible compartments [7] and more severe heat fluxes in the range of 50-250 kW/m^2 post-flashover [8–10], and exhibit longer fire durations depending on the ventilation conditions [11,12]. Hence, it is vital to address both the flammability (burning behaviour) and strength of mass timber structures simultaneously, as burning of timber influences both fire development and structural capacity.

The current method by which the fire risks of timber are addressed is covering timber with fire-protective systems [13], most commonly board-type non-combustible materials such as fire-rated plasterboard [14]. This method is usually referred to as encapsulation, with the term encapsulation linked to different performance criteria depending on the country or authority having jurisdiction, but all relating to the level of protection required to delay or prevent timber ignition and charring (assumed at approximately 300 °C) [15–18]. Nevertheless, timber loses strength and stiffness even below 100 °C, with the level of reduction depending on the loading condition of the member [19–21]. In essence, the primary purpose of encapsulation is to prevent the ignition of timber and therefore its contribution to the fire for its full duration, as well as to

This article is part of a special issue entitled: FISJ_IAFSS 2026 published in Fire Safety Journal.

* Corresponding author. School of Civil Engineering, The University of Queensland, Brisbane, Australia.
E-mail addresses: s.spyridakis@uq.edu.au (S. Spyridakis), felix.wiesner@ubc.ca (F. Wiesner), andrea.lucherini@zag.si (A. Lucherini), wenxuan.wu@uq.edu.au (W. Wu), c.maluk@damaengineers.com (C. Maluk), a.orabi@uq.edu.au (A. Orabi).

https://doi.org/10.1016/j.firesaf.2026.104711
Received 24 September 2025; Received in revised form 15 February 2026; Accepted 8 March 2026
Available online 12 March 2026

slow down the heat conducted into timber and thus the rate of strength and stiffness loss in structural timber members.

Encapsulating timber elements can be costly due to additional resources and materials required for the installation after the mass timber structure is erected on-site, thereby extending construction timelines. Additionally, encapsulation systems obscure the desirable aesthetic wood features, but more importantly, they may fail in unpredictable ways such as plasterboard fall off during a fire. Gypsum is a brittle material that may result in the partial or complete fall-off of the plasterboard layer during a fire due to the combined thermal and load effects. Several fire tests of mass timber compartments with plasterboard have recorded its fall-off within the first 30 min [5,10,22].

These challenges highlight the need to explore alternative fire protection solutions for mass timber that provide an equivalent level of protection. One such solution is intumescent coatings, which have been extensively used on structural steel to reduce its rate of temperature rise in a fire [23], thereby preventing structural members from reaching critical thresholds and enabling them to sustain the intended load. These coatings offer distinct advantages over traditional fire-protective coverings, such as reduced aesthetic impact and versatility in application, on-site or off-site [24,25]. They are often formulated to have an opaque, white-coloured finish (Fig. 1 (I)), with recent formulations resulting in the production of transparent or clear-finish coatings (Fig. 1 (II)) [26].

Opaque thin intumescent coatings are applied at thicknesses of up to 3 mm – known as Dry Film Thickness (DFT) [27,28], with the maximum DFT of transparent coatings generally not exceeding 0.4 mm. When these coatings are exposed to sufficient heat, they undergo a transient swelling process, expanding up to 50-100 times their original thickness [29,30], creating a stratified layer that insulates the substrate [31] (Fig. 1 (III)), known as the intumescent char layer. The temperature range in which this layer forms has been reported to be 200-400 °C [32], with its thermal degradation occurring as a result of oxidation between 400 and 800 °C, depending on the coating formulation and testing mechanism [32,33]. These temperature ranges are associated with the four phases of the intumescent process [34]: (1) thermal decomposition or melting, (2) reaction or swelling resulting in (3) char layer formation, and (4) char degradation due to oxidation [32,34].

Several testing methods and experimental investigations have been employed in the literature to evaluate the performance of these coatings [25,29,35,36], including simultaneous thermal analysis [37], butane torch exposure [38], and cone calorimeter testing [39]. Some of this work is also specifically concerned with the behaviour of the coating in isolation [40], or the chemistry of the material [41] rather than the performance of the overall coated system. Moreover, knowledge gaps remain regarding how variations in the intumescent coating type and DFT, as well as heat flux level and exposure duration, can impact the fire behaviour and structural fire performance of intumescent-coated mass timber structures during the different fire phases [34,42–46].

The authors have previously investigated the ability of two opaque (A, B) and one transparent (C) thin intumescent coating to delay and reduce charring in timber for different DFTs and heat flux levels [34,47], and how they compare with different plasterboard layer configurations [42,43]. The authors also investigated in Ref. [48] the fire behaviour of coated timber and its performance after swelling, with a focus on how the coating may delay timber ignition, limit flame spread, and heat release under varied heat fluxes. Unlike other fire-protective coverings such as plasterboard, intumescent coatings are a dynamic system whose efficacy as an encapsulation method changes with time, type of substrate, and heating conditions. This research study therefore examines the thermal behaviour of the three coatings (A, B, and C) at the material level (micro-scale) and system level (applied at real scale to timber), bridging the gap between coating performance as an individual material and coating behaviour when assessed as part of a system.

While the previous studies by the authors focused on the fire behaviour of coated timber and effectively its performance after swelling, this study investigates in detail the thermal behaviour of each coating individually and its effects on the timber substrate during the transient swelling process, leading to the formation of the intumescent char layer. In addition, while exploration of the fire performance of thin intumescent coatings and the coated substrate is essential for verifying their efficacy as a fire protection measure, it is also important to study the durability of these coatings under environmental factors such as moisture and sun exposure. These factors may degrade or alter the performance of intumescent coatings during the building's design life, particularly for external applications. However, this lies beyond the scope of this study and merits a separate, dedicated investigation.

2. Material and methods

2.1. Micro-scale tests

Thermo-gravimetric analysis (TGA) (Fig. 2 (a)) is used to characterise the thermal decomposition of materials by measuring the corresponding mass loss as a function of temperature rise. This, however, does not capture material physical transitions that do not involve a mass change, such as the melting phase of intumescent coatings where the solid (dry) coating physically changes to viscous fluid before it starts to swell [32,49]. This is not to say that a coincident mass loss cannot take place during melting, particularly given that acid source decomposition may take place at the temperature range for melting, but it is that the changes responsible for the phase change do not, generally, cause a change in mass. Physical transitions for phase change can instead be captured by using digital scanning calorimetry (DSC). The DSC apparatus (Fig. 2 (b)) performs calorimetry measurements by quantifying the heat flow experienced by a sample during heating, cooling, or at constant temperatures [50].

TGA and DSC thermal analyses were the basis to explain the intumescent process for all three coatings. Specifically, the thermal transition events relating to melting and swelling, including thermal decomposition events driven primarily by oxidation at higher temperatures, where key components undergo decomposition.

TGA and DSC testing was undertaken separately but using the same heating rates of 5 °C/min. The TGA samples were exposed to a temperature range of 50-800 °C in air, while the DSC samples were tested at 25-400 °C in nitrogen due to equipment limitations. Using different test atmospheres for the different tests is appropriate in this case, as the primary use of the DSC was to detect the melting phase of the intumescent coatings, which cannot be captured in TGA, and is expected to occur within the tested temperature range. It is important to note, however, that this is applicable for the kind of intumescent coatings used

Fig. 1. Coatings applied on timber: (I) Opaque, (II) Transparent, (III) Transparent swelled.

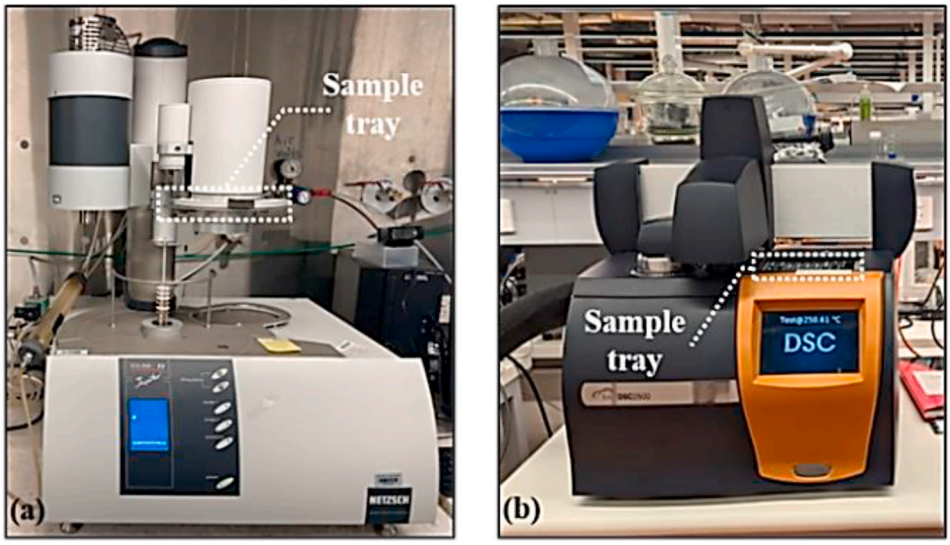

Fig. 2. Netzsch STA449-F3 (a) and TA SDT 650 (b) apparatuses used for micro-scale testing.

in this study, as shown clearly by Lucherini et al. [45]. There are other types of coating materials, such as the one discussed in Ref. [37], which can exhibit significant differences in DSC results depending on testing atmosphere. Additionally, the heating rate of 5 °C/min was selected to allow for a sufficient resolution for identifying thermal transition events. For instance, melting for coatings has been reported to occur at temperatures between 180 °C and 200 °C [32,51], preceding the onset of swelling at about 200 °C [32].

2.2. Bench-scale tests

The main purpose of the bench-scale fire tests was to identify the critical (minimum) heat flux for the onset of swelling of the coated timber samples, which corresponds to the minimum threshold at which the coating begins to insulate the timber. These bench-scale results are combined with the micro-scale (material-level) data to evaluate the thermal behaviour of the coatings at the system-level. System-level behaviour allows for identifying critical parameters for the insulating performance of intumescent coatings when applied at a real scale on timber. For bench-scale testing, a version of the Heat-Transfer Rate Inducing System (H-TRIS) [52] was used, with a detailed explanation of the setup (Fig. 3) provided in Ref. [34].

The apparatus includes an array of four moveable radiant panels, which allows imposing radiant heat fluxes in the range of 5 to 100 kW/m^2. For the bench-scale tests herein, the analyses are based on both existing test results at heat fluxes of 25, 50, and 75 kW/m^2 [34], and new test outcomes at lower fluxes to determine the critical heat flux for the onset of swelling. While the experimental setup aims to achieve, as much as practicable, a uniform heat flux over the exposed surface of the sample, inevitable discrepancies due to edge effects and the view factor between the sample and the flat radiant panel surface result in a higher net heat flux at the centre (about 10% difference in the tested configuration [32]. This is why all instrumentation, such as thermocouples and coating swelled thickness, is placed along the centreline of the sample.

The onset of swelling tests involved exposing coated Cross-Laminated-Timber (CLT) samples (200 mm × 200 mm × 110 mm) to a range of constant incident radiant heat flux levels between 8 and 20 kW/m^2. The tests were conducted in a descending heat flux order, starting at 20 kW/m^2 until the critical heat flux for swelling was identified. This approach is based on the methodology from Ref. [23] and findings from Ref. [34], where swelling occurred at 25 kW/m^2 and above regardless of coating type and DFT. Each test was terminated 5 min after swelling of the coating was observed, or after 30 min for samples that did not swell. The swelling criterion was defined as swelling at least 3 mm greater than the original DFT. The 3 mm criterion is based on the edge thickness of the sample holder used, making it possible to visually record the time-to-onset of swelling using the camera-monitor setup for samples with a minimum swelled thickness of 3 mm.

To verify the critical swelling heat flux once it was identified for each coating type, a repeat sample was tested at this heat flux, followed by two more samples at a flux level lower by 1 kW/m^2. A spark pilot ignition source was used for the whole duration of the tests to investigate whether the release of volatile gases from the coatings (typically between 200 and 300 °C [32,53]) can lead to flaming ignition on the surface of the coating, and how this could affect the intumescent char

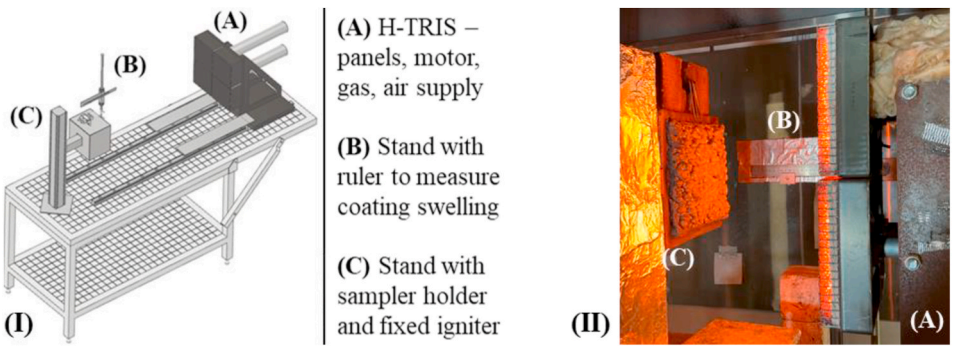

Fig. 3. H-TRIS apparatus; (I) Schematic [34]; and (II) Photo during testing of a coated sample.

layer formation. Equally, timber produces a large amount of flammable volatile gases at temperatures of 300 °C and above [54], which could also lead to ignition, subsequently affecting the coating's intumescent process.

2.3. Sample preparation

The selected intumescent coatings are commercially available for internal applications in the built environment, with Coating A (opaque, solvent-based) being a flagship product used for steel substrates. Coating B (opaque, water-based) was originally developed for concrete substrates and was modified by the manufacturer for use on timber substrates by including inorganic fibres to reduce its swelling factor. Coatings B and C have a different manufacturer from Coating A, with Coating C (water-based, transparent) intended for use on timber substrates. All coatings were applied on the front surface of the bench-scale samples using an airless spray gun with different heads depending on the coating type, with Coating C requiring a topcoat for durability purposes. Bench-scale samples for the onset of swelling tests had a mean density of 503.7 kg/m^3, with a standard deviation (SD) of ±23.1 kg/m^3 and a moisture content (MC) by weight of 9.1%, with a standard error (SE) of ±0.1%. Both density and MC for each surface type are shown in Table 1.

The mean values are based on three repetitions per coating classification for samples used to plot the onset of swelling data for heat fluxes below 20 kW/m^2, as above this flux data from Ref. [34] were used. The MC per coating classification is based on sacrificial samples following the oven drying method [55]. For consistency with the experimental data from Ref. [34], the same application method was followed herein, and three DFT levels were also applied for each coating of similar DFT ranges – Low, Medium, and High. The DFT ranges were selected so that the minimum and maximum thicknesses of the opaque coatings (A, B) fall within the same range for comparison purposes, and the DFT does not exceed 3 mm in line with typical application thickness for thin coatings. Additionally, the High DFT for the opaque coatings was based on the maximum application thickness recommended by the Coating B manufacturer. Similarly, the DFT range for transparent Coating C was selected according to the minimum and maximum ranges identified by its manufacturer. Classifying the DFT applied to the samples as Low, Medium, or High provides a qualitative means of linking the amount of applied coating to its performance.

Each bench-scale sample was drilled on its side using a CNC machine to create 2 mm holes for thermocouple (TC) insertion near the exposed surface prior to the application of the intumescent coating, following the methodology described in Ref. [34]. Type K Ø1.5 mm TCs (sheathed) were inserted at 3 mm and 5 mm from the exposed surface to track the temperature of the timber near the coated substrate during swelling. Placing TCs from the side was done to minimise thermal bridging effects [56,57]. To approximate one-dimensional heat transfer expected in full-sized CLT panels, each sample was wrapped using ceramic fibre paper and aluminium foil (Fig. 4 (i)). All micro-scale samples were prepared from spare bench-scale samples, with three repeats conducted per coating type. For each coating tested in TGA and DSC, a blade was used to obtain shavings from the dried coated surface of timber samples (Fig. 4 (ii)), which were then finely sectioned. The same spare bench-scale sample was used for each category, such that all crucibles contained material obtained from the same source across both apparatuses, enabling more precise comparison. For the TGA tests, samples weighed 9.7 ± 0.2 mg and were placed in alumina open-lid crucibles, while the DSC samples weighed 2.5 ± 0.1 mg and were placed in closed-lid crucibles with a pinhole, allowing gases to be released and preventing pressure build-up.

Table 1
Coating DFT classification, timber density and moisture content coated timber samples.

Surface Type	Opacity	Thickness Classification	DFT [mm]	Density [kg/m^3]	MC [%]
Coating A	Opaque	Low	1.16 ± 0.14	489.3	9.2
		Medium	1.63 ± 0.17	496.8	9.4
		High	2.42 ± 0.18	526.4	9.1
Coating B		Low	1.09 ± 0.11	496.2	9.0
		Medium	1.75 ± 0.10	513.5	8.7
		High	2.23 ± 0.13	504.5	8.8
Coating C	Transparent	Low	0.18 ± 0.02	512.6	9.4
		Medium	0.27 ± 0.02	494.7	9.4
		High	0.36 ± 0.04	499.5	9.1

3. Results and discussion

3.1. Intumescent coatings material characterisation

The TGA and DSC test results for coatings A, B, and C, are presented in Figs. 5–7, respectively. The temperatures linked to key reaction peaks and corresponding intumescence ranges are also presented. Each TGA plot presents the thermogravimetric (TG – normalised mass) and DTG (derivative of TG) curve, with all repeats shown for each curve. For the DSC data, the mean heat flow curve is plotted in addition to the individual curve of each of the three samples. While there were variations in heat flow peak magnitudes among the curves of repeated samples in DSC, the curves had consistent temperature thresholds. The large variance in peak magnitude limits the quantification of the enthalpy of main thermal transition events in DSC, however, the consistency in heat flow change thresholds enables the clear identification of the associated temperatures ranges. Hence, this allowed correlation of the derived thermal events in DSC with key reactions in TGA to define the main physical transitions associated with the formation of the intumescent char layer.

Combining the TGA and DSC data for each coating, the thermal decomposition events associated with the first three phases of the intumescent process can be classified into two groups (Table 2): (1) melting – acid and carbon source, and (2) swelling and intumescent char layer formation – the interaction of the acid and carbon sources with the blowing agent, releasing gases causing the coating to expand. Overall, the melting phase for Coating C occurred about 50 °C lower than coatings A and B, while char layer formation was completed by approximately 415 °C for all three coatings, indicated by a quasi-plateau in the TG and DTG curves (between 400 and 450 °C).

Based on existing literature, melting for intumescent coatings is in the range of 180 °C and 200 °C [32,51], with inorganic acids reacting at 100-250 °C [27,58], while swelling and intumescent char layer formation take place at approximately 200-400 °C [32]. For instance, carbonisation of the char agent typically occurs below 280 °C, and between 280 °C and 350 °C, the decomposition of the blowing agent generates gaseous products, causing the char layer to expand, with this process completed by 430 °C – a point where the thermal conductivity of the coating has decreased, thus the insulation to the substrate increased [27,58]. Therefore, the empirically derived temperatures for all three coatings are within the expected range reported in the literature.

Furthermore, a third DTG peak, unique to Coating C, was observed at 385 °C (between 375 °C and 415 °C). This is attributed to an early-stage oxidative reaction, as the onset of oxidation in coatings has been reported at temperatures above 400 °C [32,33]. As evidenced by the TG data, Coating C also exhibited the most mass loss (~60%) during swelling and char layer formation, followed by Coating A (~40%) and Coating B (~30%). Based on these results, it is deduced that Coating C involved the loss of more mass in forming the intumescent char layer than coatings A and B, suggesting a lower content of inorganic compounds. The oxidation phase for each coating is further evaluated below based on the full TGA temperature range (between 50 °C and 800 °C). For ease of comparison, the mean TG and DTG curves are plotted in Fig. 8, with key DTG (oxidation) events marked, while the full TGA results with repeat tests per coating type are provided in Appendix A

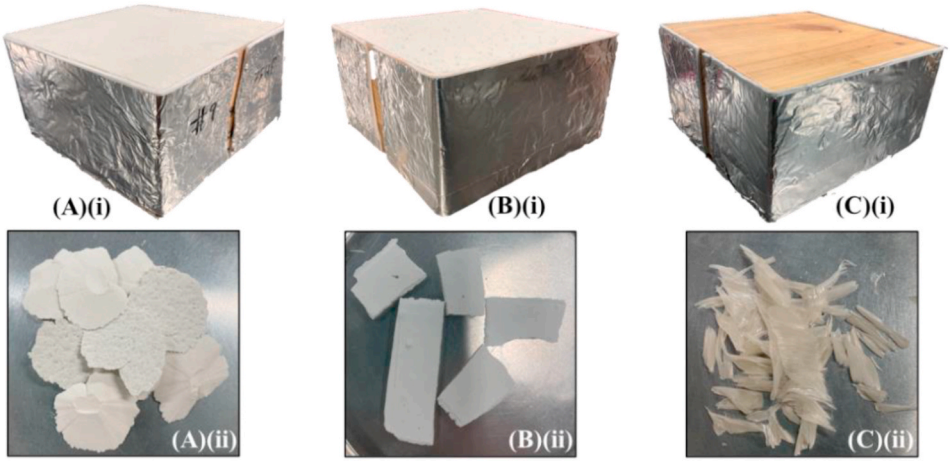

Fig. 4. Bench-scale (i) and micro-scale (ii) samples for: (A) Coating A, (B) Coating B, and (C) Coating C. *Note:* Micro-scale material shown before sectioning and bench-scale samples include insulation wrapping with an open section for in-depth thermocouples.

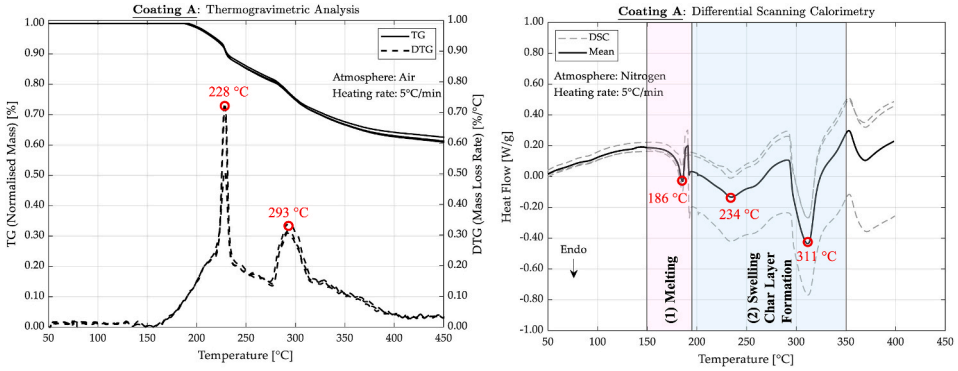

Fig. 5. TG and DTG curves from TGA and DSC curves with mean for Coating A samples.

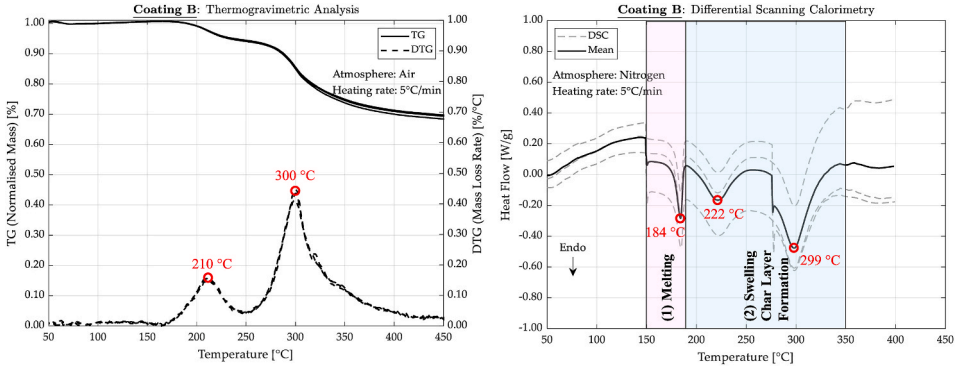

Fig. 6. TG and DTG curves from TGA and DSC curves with mean for Coating B samples.

(Fig. A1).

At post-swelling temperatures (>450 °C), coatings A and C experienced an additional 20% mass loss during oxidation by the end of the heating cycle (800 °C), while Coating B underwent an additional 15% mass loss. Hence, the residual mass (inorganic content) of transparent Coating C (21%) by 800 °C was less than half that of the opaque coatings – A (43%) and B (55%). The DTG peaks within the 450-800 °C oxidation range are small relative to the peaks during swelling and intumescent char layer formation, and are within the temperature range associated with the oxidation of the char layer previously reported in the literature [32,33,45].

Although all coatings exhibited similar levels of mass loss post-swelling, the residual mass of Coating C markedly deviated from A and B due to its early oxidation at approximately 385 °C, which resulted in Coating C losing 20-30% more mass than A and B before 450 °C. The early-stage oxidation for the transparent coating, likely caused by its lower inorganic content, indicates reduced thermal durability of its intumescent char layer and thus reduced insulating performance at system level compared to the opaque coatings. This poses a limitation of Coating C, providing meaningful passive fire protection for mass timber, particularly in a fully developed fire (post-flashover), where heat flux levels exceed 50 kW/m^2 [59] and compartment ceiling temperatures rise above 600 °C [60,61].

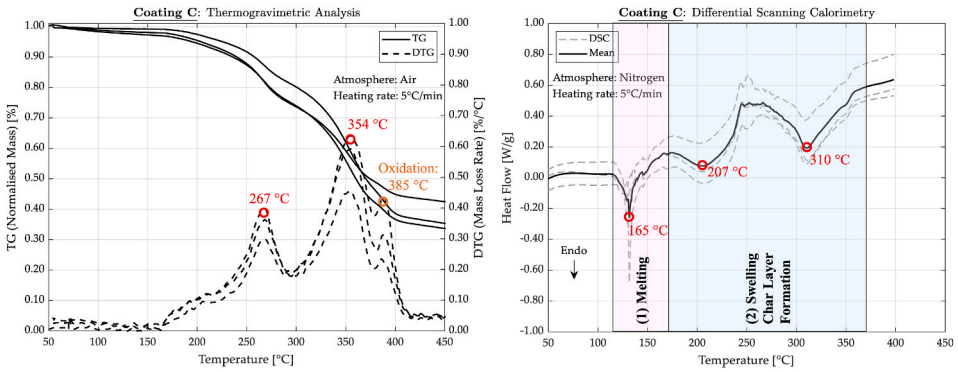

Fig. 7. TG and DTG curves from TGA and DSC curves with mean for Coating C samples.

Table 2
Thermal decomposition events, key reactions, and temperature ranges for each coating.

Thermal Decomposition Groups	Intumescence Events	Key Reaction Peaks and Corresponding Ranges		
		Coating A [°C]	Coating B [°C]	Coating C [°C]
(1): Melting 115-195 °C	Thermal decomposition	P: 186 D: 150-195	P: 184 D: 150-190	P: 132 D: 115-165
(2) Swelling Char Layer Formation 165-415 °C	Release of gaseous products	P: 231 ± 3 T: 165-275 D: 195-294	P: 216 ± 6 T: 165-250 D: 190-278	P: 237 ± 30 T: 165-295 D:165-270
	Char structure development	P: 302 ± 9 T: 275-415 D: 294-350	P: 299 ± 1 T: 250-415 D: 278-350	P: 332 ± 22 T: 295-415 D: 270-370

Note: **P:** Key reaction peak temperature; **T:** DTG temperature range; **D:** DSC temperature range.

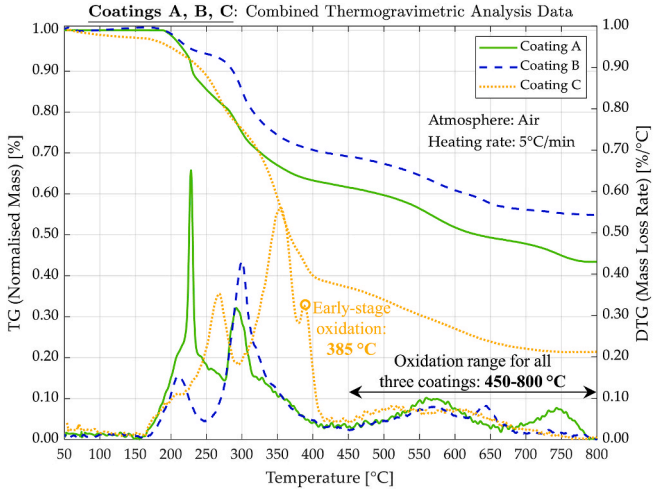

Fig. 8. Combined TGA data (mean TG and DTG curves) for coatings A, B, and C at 50-800 °C.

3.2. Onset of swelling conditions for coated timber

The previous section characterised the thermal behaviour of all three intumescent coating materials from their intumescence and oxidation events. This section evaluates the system-level behaviour of the coatings when applied on timber, combining the micro-scale findings with bench-scale results with 1D heating conditions. Specifically, it defines the minimum conditions for the onset of swelling, while the next section examines the timber's thermal behaviour at the end of transient swelling – i.e., the peak thermal insulation. The time-to-onset of swelling for each coating at different heat fluxes is shown in Fig. 9 (I-III), accounting for all three DFT levels and identifying the critical heat flux (CHF).

The CHF for onset of swelling was observed at 13 kW/m^2 for opaque Coating B and 10 kW/m^2 for transparent Coating C, irrespective of DFT level. However, for Coating A High DFT coated timber samples, the onset of swelling was first recorded at 15 kW/m^2, as opposed to Low and Medium DFT samples at 13 kW/m^2. A similar increase in DFT from Low to High did not affect the onset of swelling flux for Coating B and C samples. The correlation between DFT and CHF observed for A is likely due to its overall thicker coated surface than B and C. Ultimately, a higher critical swelling heat flux indicates additional required heat to reach the activation temperature for the coating to fully transition from the melting phase to the initiation of transient swelling. The CHF for onset of swelling for the opaque coatings (A, B) was thus in the range of 13-15 kW/m^2, while for transparent Coating C it was 10 kW/m^2.

Past experimental studies on an opaque intumescent coating product, similar to opaque coating A but applied on steel, reported a CHF range of 20-23 kW/m^2 [23,32]. The 5-10 kW/m^2 lower CHF for the timber substrate in this study is attributed to the lower thermal inertia of timber compared to steel, which results in reduced heat losses at the coating-substrate interface, enabling faster temperature increase of the coating at lower heat fluxes. In contrast, steel acts as a heat sink, resulting in high heat losses at the back of the coating (i.e., the interface with the substrate), slowing its expansion and requiring more time to reach swelling reaction temperatures.

All coatings began to swell in under a minute for heat fluxes at and above 50 kW/m^2, with Coating A swelling in about 2 min at 25 kW/m^2 and coatings B and C within 1 min. In contrast, opaque coatings A and B took about 10-11 min to begin swelling at their critical heat flux thresholds and Coating C approximately 10 min, irrespective of DFT levels. The time-to-swell for all three coatings at those heat fluxes was much shorter than values reported for steel substrates [23,32]. Overall, the coating DFT level had a negligible impact on the time-to-swell – particularly at heat fluxes of 25 kW/m^2 and above, with time-to-swell instead being inversely proportional to the applied heat flux and influenced by the type of substrate. The CHF values for the coated timber samples were also compared with the critical flux for piloted ignition of bare timber (15 kW/m^2) that was obtained from ignition testing on uncoated samples. The CHF for coating activation was found to be less or equal to the CHF for the ignition of the timber. This suggests that coated

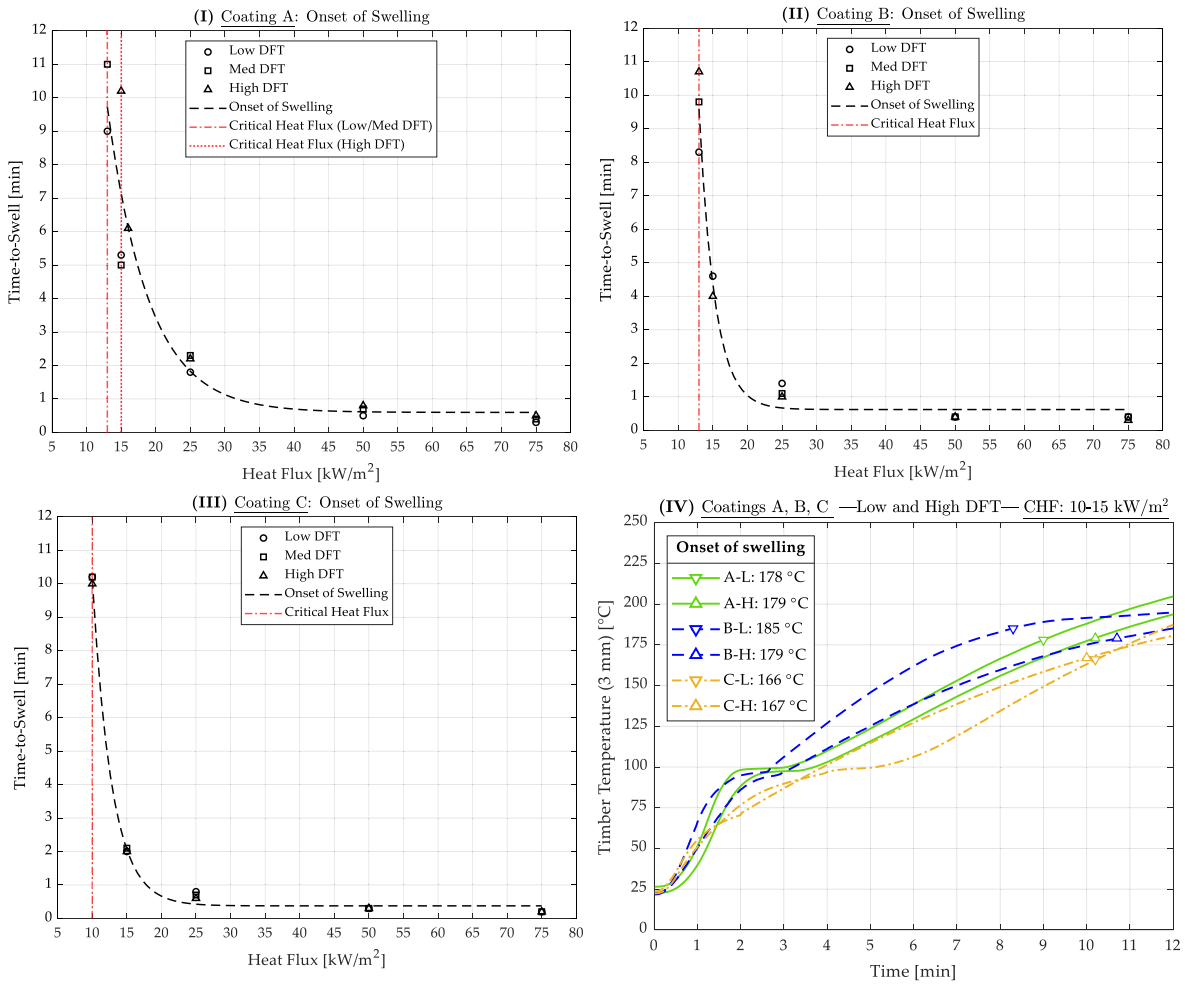

Fig. 9. Heat flux level vs. time-to-swell (I-III) for coated timber samples of coatings A, B, and C, and timber temperature at 3 mm from the surface (IV) for the critical onset-of-swelling fluxes. *Note:* Different line styles in (IV) represent coating type and marker style Low or High DFT.

timber is unlikely to reach critical temperatures for ignition behind the coating surface at the CHF levels required for coating activation. It can thus be concluded that the tested intumescent coatings can activate early in a fire during the developing phase, where heat flux levels below 20 kW/m^2 are typically present [14,61], thereby delaying or preventing timber ignition.

The in-depth timber temperature evolution at 3 mm for each coating at the CHF for the onset of swelling is also plotted in Fig. 9 (IV) for Low and High DFTs, providing an upper and lower bound threshold for defining the temperature at the onset of swelling. This provides a means to assess the level of thermal degradation in coated timber prior to the coating beginning to insulate the substrate. The CHF values were selected because the slower heating rates made temperature thresholds easier to identify. These temperatures were measured at 3 mm rather than at the timber-coating interface because 2 mm TC holes were created from the side to minimise thermal bridging and could not be placed closer to the surface. However, the 3 mm measurement is expected to provide a reasonable approximation of the surface temperature. At the onset of swelling, the coated timber temperature at 3 mm was measured as: 177 ± 1 °C (Coating A), 182 ± 3 °C (Coating B), and 165 ± 1 °C (Coating C). While these temperatures are within the range previously reported in the literature (90-260 °C [23]) for steel substrates with a coating type and DFT levels similar to Coating A, the key question lies in the thermal behaviour of the substrate when evaluating the feasibility of intumescent coatings as a fire protection method for mass timber.

For structural steel, significant strength loss typically occurs at temperatures above 400 °C [62]; therefore, the aforementioned temperature values at the onset of swelling for each coating would not be of concern for the design of steel structures. However, timber loses strength below 100 °C, with permanent reductions reported at 65 °C [63,64]. By around 200 °C, strength reductions become severe and vary with the loading conditions of the structural timber member [19,21,65]. For instance, timber loses approximately 90% of its strength in compression by 200 °C and nearly 70% in tension, with temperatures of 300 °C and above associated with zero strength [20]. Additionally, timber pyrolysis and thus the thermal decomposition of key organic components in timber occur at temperatures between 200 and 300 °C and above [14,54,66].

Furthermore, timber has low thermal conductivity compared to steel [61,66], which results in large internal temperature gradients with the outside layer insulating the inside thus allowing it to retain residual strength. However, if the portion of timber near the surface reaches temperatures close to 200-300 °C before the coating begins to insulate it, then the loadbearing capacity of that region is effectively lost. If the remaining timber stays relatively cool, then its strength reductions are limited, and the "core" of the member could retain considerable residual strength. Hence, the timber surface and overall member temperature profile at the end of transient swelling becomes a design consideration for mass timber structures. This is investigated in detail in the following section for heat fluxes above the onset of swelling CHF, where transient swelling was completed.

3.3. Coated timber thermal profile at the end of swelling

Test data from Ref. [34] are utilised herein to derive the temperature of the timber when the intumescent char layer is formed, which is associated with the end of transient swelling and thus the maximum insulating effect. To achieve this, the time at which swelling is completed and the corresponding in-depth temperature of the coated timber near the surface (3 mm) were first obtained, followed by the overall timber temperature to assess its level of degradation. As seen in Fig. 10, the coated timber temperature at 3 mm over time is differentiated by coating type, accounting for Low and High DFTs, and exposure to 25 kW/m^2 and 75 kW/m^2 for 60 min. Samples of Medium DFT and those exposed to 50 kW/m^2 were not considered here for ease of comparison, as the purpose is to define an upper and lower limit for the temperature at which transient swelling is considered completed.

The end of the transient swelling process for the coated timber samples in Fig. 10 was defined as a quasi-plateau in temperature at 150-250 °C, as swelling was previously demonstrated to begin at around 200 °C close to the timber surface (3 mm). Considering the insulating effect of the coating, and thus the reduction in the rate of temperature rise in timber, the temperature after onset should not vary significantly until the intumescent char layer begins to oxidise and lose integrity. Indeed, the timber temperature range at 3 mm for the "High DFT – 25 kW/m^2" condition remained within approximately 200-250 °C for coatings A (10-25 min) and B (15-35 min), and about 150-250 °C for Coating C (10-20 min).

For Low DFTs – regardless of heat flux and coating type – a quasi-plateau around 150-250 °C for the first 10-30 min could not be observed, particularly for Coating C timber samples, including those with High DFT at 75 kW/m^2. As a result, under these conditions, all three coatings would begin to thermally degrade before the transient swelling process is completed, with Coating C's High DFT swelling being overtaken by rapid degradation of the intumescent char later after approximately 20 min at 25 kW/m^2. In fact, it was previously demonstrated by the authors that the insulating efficacy (measured as reduction in charring) of Coating C significantly reduced at heat fluxes above 25 kW/m^2, regardless of DFT level [34]. The degradation of Coating C's (High DFT) intumescent char layer at 25 kW/m^2 over time is illustrated in Fig. 11, with photos from a representative charring test at selected intervals during the 60-min exposure.

Based on the above findings, to derive the timber temperature at the completion of swelling, the mean temperature at 3 mm for the High DFT samples at 25 kW/m^2 is plotted in Fig. 12 (I). For this condition, the first 40 min of exposure are shown, due to the slower rate of degradation observed in all three coatings. In addition, the rate of temperature change (i.e., slope) at 3 mm was calculated from the mean values and is plotted in Fig. 12 (II) at 5-min intervals for each coating. These slopes highlight the incremental change in temperature at 3 mm across successive intervals, to further support the findings associated with the coatings' insulating effects during and at the end of transient swelling.

Furthermore, the time, and the temperature for the coatings when they completed their transient swelling process, or when this was interrupted by degradation of the coatings, are marked on both plots in Fig. 12. The criteria for this were the visual observation of the swelled coating ceasing to expand and retaining its swelled thickness for at least 1 min, or beginning to retract (i.e., decrease in thickness) during swelling due to thermal degradation. As indicated in Fig. 12 (I), the end of transient swelling for Coating A occurred at 19 min, corresponding to a timber temperature at 3 mm of 244 ± 8 °C, while for Coating B this occurred at a similar temperature – i.e., 221 ± 6 °C at 26 min. However, the swelling for Coating C was disrupted by its thermal degradation at approximately 18 min, with the timber temperature in the range of 201 ± 23 °C. These observations are further supported by the 5-min temperature slopes shown in Fig. 12 (II), where the end of swelling for opaque coatings A and B is marked by a temperature rise plateau of 2 °C/min. In contrast, transparent Coating C was affected by thermal degradation of the already swelled layer, as evidenced by the increase in the rate of temperature rise after 20 min exceeding 5 °C/min.

Since the end of swelling was identified within 20-30 min, the overall timber temperature at this point was plotted to infer its thermo-mechanical performance, as shown in Fig. 13 (I). For comparison purposes, in-depth temperature for bare timber is also presented, based on the test data from Ref. [34]. It can be seen from Fig. 13 (I) that by 30 min the temperature of the timber at 20 mm and deeper from the coating-timber interface was below 100 °C, and temperatures at 15 mm ranged 100 °C and 150 °C for all three coatings. Additionally, only for the first 10 mm the in-depth timber temperature for coatings A and C exceeded 200 °C, while for Coating B it remained at about 150 °C. Accordingly, for all three coatings the heated region of timber within the first 15-20 mm from the coated surface can be considered to have severely reduced mechanical properties by the end of the swelling process, with the remaining timber retaining most of its original strength.

The temperature profiles at 60 min are presented separately in Fig. 13 (II) to assess the timber's residual strength post-swelling. The timber region that remained below 200 °C by 60 min was at a depth of about 20 mm for Coating A, 15 mm for Coating B, and 25 mm for Coating C, whereas for bare timber this was at about 55 mm. In addition, the temperature for all coated timber samples from 30 to 35 mm (interface of first and second lamellas) and deeper remained below 100 °C, while for bare timber it did not drop below 100 °C until a depth of about 60-65 mm. Therefore, the in-depth timber temperature profile for coatings A and B progressed minimally by 60 min, while it advanced significantly for Coating C and bare timber samples.

Combining the temperature results of plots (I) and (II) in Fig. 13, there is an evident loss of strength in the timber for all three coatings during transient swelling, before the timber can be considered fully insulated. Further deterioration for coatings A and B was minimal compared to Coating C due to the early thermal degradation of its intumescent char layer. Indeed, while strength loss in coated timber occurred during the intumescent char layer formation irrespective of coating type, DFT, or heat flux level and exposure time, the extent of deterioration post-swelling has previously been shown by the authors to depend on these parameters [34].

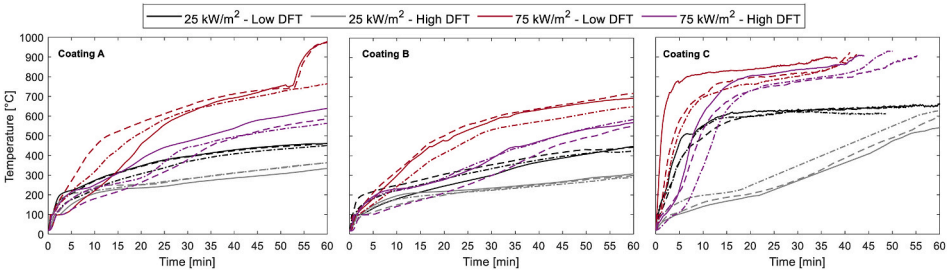

Fig. 10. Coated timber in-depth (3 mm) temperature evolution for Low and High DFT samples, exposed to 25 kW/m^2 or 75 kW/m^2 for 60 min. Different line styles represent repeat samples.

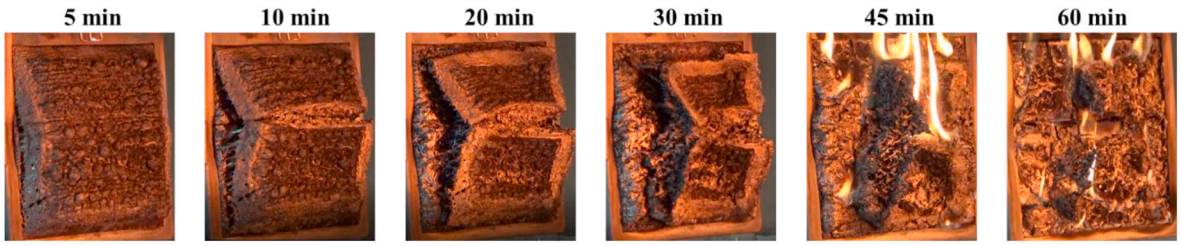

Fig. 11. Thermal degradation at different times for a Coating C High DFT sample at 25 kW/m^2.

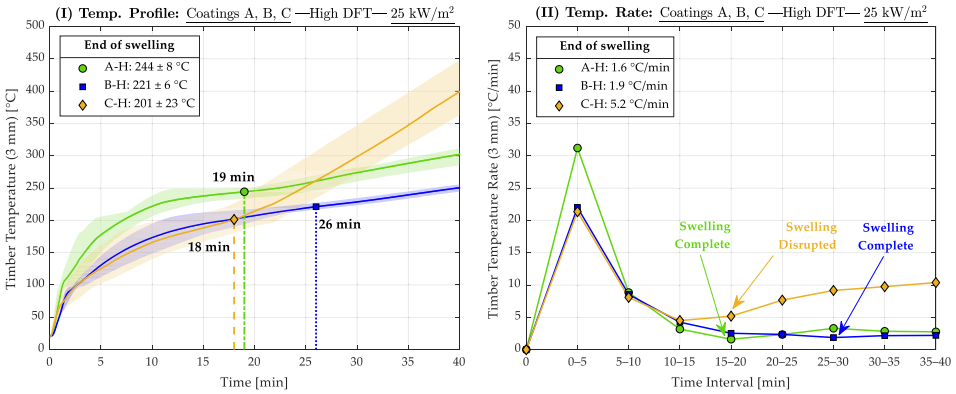

Fig. 12. Coatings A, B, C (High DFT) timber (I) temperature (3 mm) and (II) rate at 25 kW/m^2. *Note:* The mean is shown as a solid line, with shading representing the maximum and minimum.

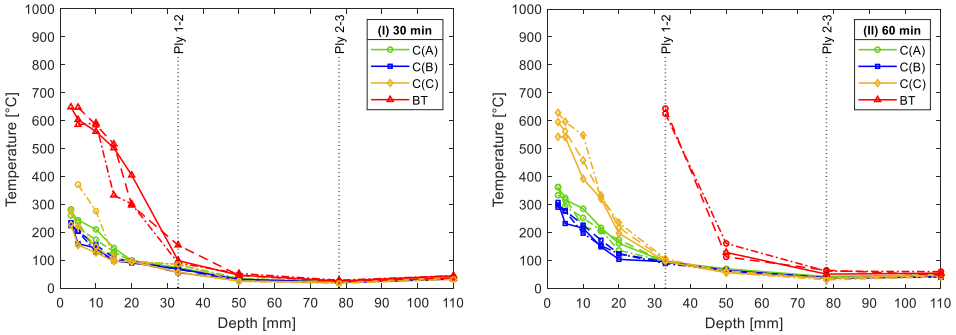

Fig. 13. In-depth timber temperature at (I) 30 min and (II) 60 min for coated (High DFT) and bare samples a 25 kW/m^2. Line styles refer to repeat samples, and ply to lamella intersection.

It can be concluded that for the design of intumescent-coated mass timber in fire, a reduction in the timber's loadbearing capacity should be considered not only after the intumescent char layer has formed, but also earlier during the transient swelling process – irrespective of coating type, DFT, or exposure conditions. Unlike board-type fire-protective coverings such as plasterboard, where protection of the timber is assumed from the onset of the fire, the insulating benefit of intumescent coatings develops in a dynamic manner. This consideration is particularly pertinent for CLT slabs, depending on the lamella thickness. When strength is lost in the first lamella, the cross-layer (second lamella) no longer contributes to the loadbearing capacity due to its grain orientation and position in the section – e.g., it cannot carry load in bending. As a result, the combined effect of the 15-20 mm heat-affected region and subsequent charring could lead to faster loss of structural capacity in CLT slabs at the early stages of a fire.

4. Conclusions

The results suggest that for the intumescent coatings and conditions tested, there were critical observations regarding the thermal behaviour of opaque and transparent coatings at both material level (micro-level) and system level (coating applied at real scale on timber), and their effects on timber. From these analyses, the following key observations are drawn:

- Although transparent Coating C begins its intumescent process at lower temperatures than the opaque coatings (A, B), it completes this process at a similar temperature range (400-450 °C). In addition, Coating C's residual mass was approximately 20% at 800 °C, while Coating A retained more than 40% and B over 50% of their initial mass. The residual mass of Coating C differed markedly from coatings A and B due to early-stage oxidation at 350-400 °C, which caused additional mass loss during intumescence, whereas the opaque coatings only underwent oxidation above 450 °C. These characteristics pose a limitation for its insulating performance at system level, particularly in a fully developed fire.
- Based on the system-level findings for the onset of swelling, the critical swelling heat flux for coatings A and B was 13-15 kW/m^2, and

10 kW/m^2 for Coating C, accounting for Low to High DFT levels. These heat flux ranges are lower than those previously reported for opaque coatings on steel (20-23 kW/m^2). This was attributed to the lower thermal inertia of timber compared to steel, resulting in reduced heat losses at the coating-substrate interface. The contrast of these swelling heat flux thresholds with the critical heat flux for ignition affirms that these coatings will activate during the developing phase of a fire, where fluxes below 20 kW/m^2 are typically present, thereby delaying or preventing the ignition of timber.

- The temperature of the coated timber samples near the interface with the coating (3 mm) at the onset of swelling was about 180 °C for coatings A and B and close to 170 °C for Coating C. In addition, at the end of transient swelling, the in-depth timber temperature at 10 mm exceeded 200 °C for coatings A and C and remained at approximately 150 °C for Coating B, while at 15 mm the temperature did not exceed 100-150 °C, and at 20 mm it was below 100 °C for all three coatings. For design purposes, a reduction in the coated timber's loadbearing capacity should therefore be considered by the end of swelling.
- The end of swelling could be defined either as the point where the coating reaches its maximum expected thickness and ceases to expand, or where swelling is interrupted by degradation of the already swelled layer. Based on the measured temperature profiles, the heated region of timber within the first 15-20 mm from the coating-timber interface could be considered to have negligible loadbearing capacity, which is directly attributed to the transient swelling process irrespective of coating type and DFT. However, the extent of deterioration in timber post-swelling will depend on these parameters.

This study used fundamental experimental techniques to investigate the fire performance of thin intumescent coatings and quantify their intumescent process both individually and when applied on timber. From this, it was found that opaque and transparent coatings have significantly different durability under heating due to the lower inorganic content of the transparent coating, resulting in an early-stage oxidation reaction that reduces its mass and negates its ability to insulate the timber.

From these findings, along with data on the temperature through the depth of the coated timber, it was demonstrated that there is a heat-affected region of timber at the end of the transient swelling process, the point where coatings are expected to provide maximum insulation. More importantly, this shows that intumescent coatings are dynamic fire protection systems, whereby the insulation provided is progressive rather than immediate, unlike board-type systems such as plasterboards, where protection is assumed from the onset of the fire.

Together with previous findings by the authors and others on intumescent-coated timber, this work provides an avenue for the future development of a practical and representative design procedure that accounts for the transience of the various thermal events expected in intumescent-coated mass timber structures.

CRediT authorship contribution statement

Stavros Spyridakis: Writing – original draft, Visualization, Project administration, Methodology, Investigation, Formal analysis, Data curation, Conceptualization. **Felix Wiesner:** Writing – review & editing, Supervision, Project administration, Methodology, Conceptualization. **Andrea Lucherini:** Writing – review & editing, Methodology, Conceptualization. **Wenxuan Wu:** Writing – review & editing, Methodology, Investigation, Conceptualization. **Cristian Maluk:** Funding acquisition, Conceptualization. **Anwar Orabi:** Writing – review & editing, Supervision, Resources, Project administration, Methodology, Funding acquisition, Conceptualization.

Declaration of competing interest

The authors declare that they have no known competing financial interests or personal relationships that could have appeared to influence the work reported in this paper.

Acknowledgements

The authors would like to acknowledge the financial support provided by ARC DP190102992, and thank XLam Australia, Permax Australia, and Aithon Ricerche for their support with the provision of testing material. The authors also wish to extend their gratitude to the Fire Safety Engineering Group and the technical staff in the School of Civil Engineering at The University of Queensland for their valuable assistance with testing preparations, particularly Dr Sergio Zarate, Mr Jeronimo Carrascal, Mr Stewart Matthews, Mr Shane Walker, and Mr Fraser Reid. Dr Lucherini would also like to gratefully acknowledge the financial support for the FRISSBE project within the European Union's Horizon 2020 research and innovation programme (GA 952395).

Appendix A

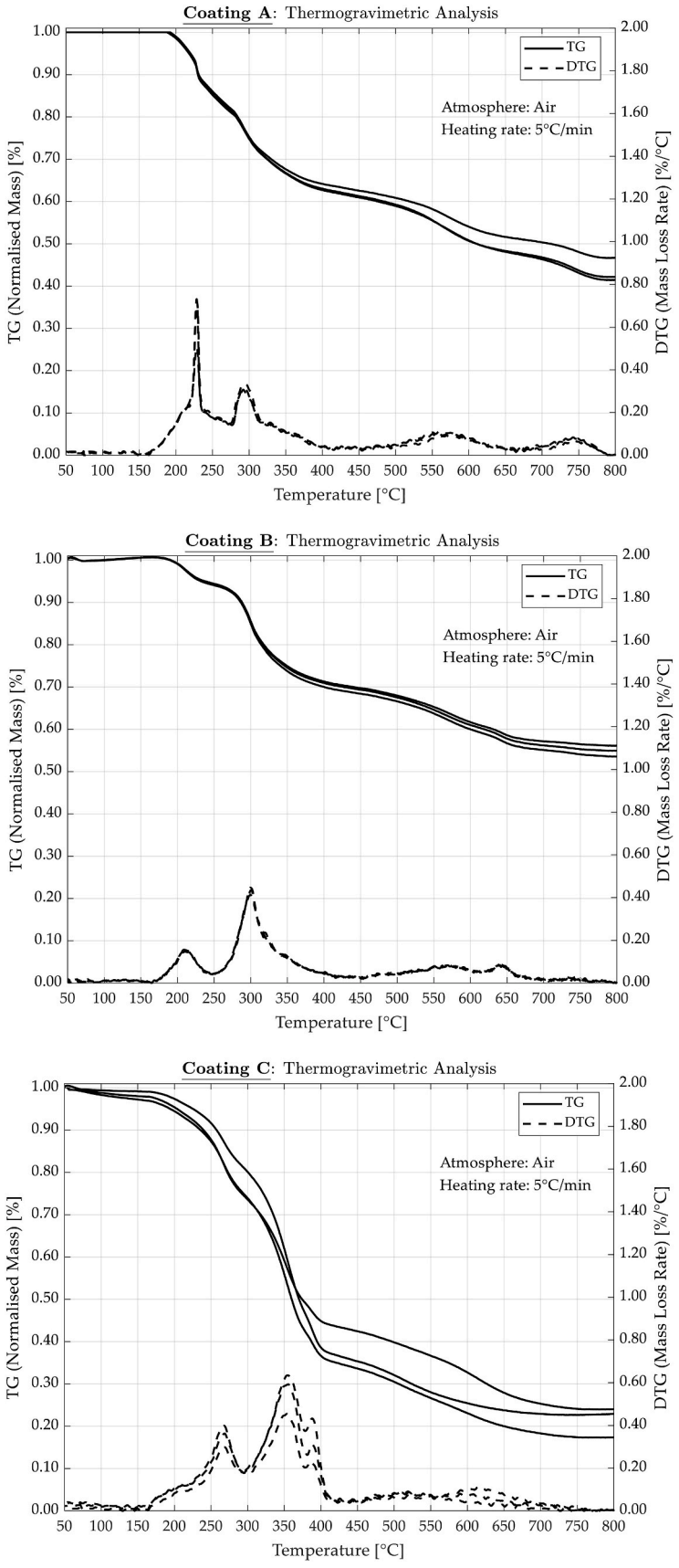

Fig. A1. TGA results (TG-solid lines and DTG-dashed lines) with repeats for all three coatings.

References

[1] D. Barber, Tall timber buildings: what's next in fire safety? Fire Technol. 51 (6) (2015) 1279–1284, https://doi.org/10.1007/s10694-015-0497-7.

[2] R. Sathre, L. Gustavsson, Using wood products to mitigate climate change: external costs and structural change, Appl. Energy 86 (2) (2009) 251–257, https://doi.org/10.1016/j.apenergy.2008.04.007.

[3] O.A. Hassan, C. Johansson, Glued laminated timber and steel beams: a comparative study of structural design, economic and environmental consequences, J. Eng. Des. Technol. 16 (3) (2018) 398–417, https://doi.org/10.1108/JEDT-12-2017-0130.

[4] N. Winchester, J.M. Reilly, The economic and emissions benefits of engineered wood products in a low-carbon future, Energy Econ. 85 (2020) 104596, https://doi.org/10.1016/j.eneco.2019.104596.

[5] R.M. Hadden, et al., Effects of exposed cross laminated timber on compartment fire dynamics, Fire Saf. J. 91 (2017) 480–489, https://doi.org/10.1016/j.firesaf.2017.03.074.

[6] P. Kotsovinos, et al., Fire dynamics inside a large and open-plan compartment with exposed timber ceiling and columns: codered# 01, Fire Mater. (2022), https://doi.org/10.1002/fam.3049.

[7] H. Mitchell, P. Kotsovinos, F. Richter, D. Thomson, D. Barber, G. Rein, Review of fire experiments in mass timber compartments: current understanding, limitations, and research gaps, Fire Mater. 47 (4) (2023) 415–432, https://doi.org/10.1002/fam.3121.

[8] S.L. Zelinka, L.E. Hasburgh, K.J. Bourne, D.R. Tucholski, J.P. Ouellette, V. Kochkin, Compartment fire testing of a two-story mass timber building, in: Geneneral Technical Report FPL-GTR-247, U.S. Department of Agriculture, Forest Service, Forest Products Laboratory, 2018.

[9] I. Pope, et al., Fully-developed compartment fire dynamics in large-scale mass timber compartments, Fire Saf. J. 141 (2023) 104022, https://doi.org/10.1016/j.firesaf.2023.104022.

[10] F. Wiesner, et al., Large-scale compartment fires to develop a self-extinction design framework for mass timber-part 2: results, analysis and design implications, Fire Saf. J. (2025) 104346, https://doi.org/10.1016/j.firesaf.2025.104346.

[11] F. Wiesner, et al., Structural capacity of one-way spanning large-scale cross-laminated timber slabs in standard and natural fires, Fire Technol. 57 (1) (2021) 291–311, https://doi.org/10.1007/s10694-020-01003-y.

[12] P. Kotsovinos, et al., Impact of ventilation on the fire dynamics of an open-plan compartment with exposed timber ceiling and columns: codered# 02, Fire Mater. 47 (4) (2023) 569–596, https://doi.org/10.1002/fam.3082.

[13] International Code Council and SFPE, Fire Safety for Very Tall Buildings: Engineering Guide, Springer, 2022.

[14] A. Buchanan, B. Östman, Fire Safe Use of Wood in Buildings: Global Design Guide, Taylor & Francis, 2022.

[15] Violette, Memoir on the charcoals of wood, Ann. Chem. Phys. 32 (1851) 20–74 [Online]. Available: https://gallica.bnf.fr/.

[16] E.L. Schaffer, Charring Rate of Selected woods-transverse to Grain, vol. 69, USDA Forest Service, Forest Products Laboratory, Madison, WI, 1967. FPL.

[17] R. White, Charring Rates of Different Wood Species, University of Wisconsin-Madison, Madison, WI, 1988. Ph.D.

[18] R.H. White, Charring rate of composite timber products, in: Wood & Fire Safety (WFS 2000), 2000, pp. 353–363.

[19] F. Wiesner, et al., Structural capacity in fire of laminated timber elements in compartments with exposed timber surfaces, Eng. Struct. 179 (2019) 284–295, https://doi.org/10.1016/j.engstruct.2018.10.084.

[20] Eurocode 5, *Design of Timber Structures – Part 1-2: General –Structural Fire Design*, EN 1995-1-2, 2004, ed. 2004.

[21] E. Garcia-Castillo, T. Gernay, I. Paya-Zaforteza, Probabilistic models for temperature-dependent compressive and tensile strengths of timber, J. Struct. Eng. 149 (2) (2023) 04022239, https://doi.org/10.1061/JSENDH.STENG-11369.

[22] M. Hevia, A. Ramon, Fire Resistance of Partially Protected cross-laminated-timber Rooms, Carleton University, Ottawa, 2014. M.App.Sc., Civil Engineering.

[23] A. Lucherini, C. Maluk, Assessing the onset of swelling for thin intumescent coatings under a range of heating conditions, Fire Saf. J. 106 (2019) 1–12, https://doi.org/10.1016/j.firesaf.2019.03.014.

[24] R.G. Puri, A. Khanna, Intumescent coatings: a review on recent progress, J. Coating Technol. Res. 14 (1) (2017) 1–20, https://doi.org/10.1007/s11998-016-9815-3.

[25] A. Lucherini, C. Maluk, Intumescent coatings used for the fire-safe design of steel structures: a review, J. Constr. Steel Res. 162 (2019) 105712, https://doi.org/10.1016/j.jcsr.2019.105712.

[26] L. Yan, Z. Xu, D. Liu, Synthesis and application of novel magnesium phosphate ester flame retardants for transparent intumescent fire-retardant coatings applied on wood substrates, Prog. Org. Coating 129 (2019) 327–337, https://doi.org/10.1016/j.porgcoat.2019.01.013.

[27] S. Bourbigot, S. Duquesne, Fire retardant polymers: recent developments and opportunities, J. Mater. Chem. 17 (22) (2007) 2283–2300, https://doi.org/10.1039/b702511d.

[28] A. Lucherini, L. Giuliani, G. Jomaas, Experimental study of the performance of intumescent coatings exposed to standard and non-standard fire conditions, Fire Saf. J. 95 (2018) 42–50, https://doi.org/10.1016/j.firesaf.2017.10.004.

[29] T. Mariappan, Recent developments of intumescent fire protection coatings for structural steel: a review, J. Fire Sci. 34 (2) (2016) 120–163, https://doi.org/10.1177/0734904115626720.

[30] A.P. Taylor, F.R. Sale, Thermal analysis of intumescent coatings, Eur. Polym. Paint Colour J. 182 (4301) (1992) 122–130.

[31] M. Gillet, L. Autrique, L. Perez, Mathematical model for intumescent coatings growth: application to fire retardant systems evaluation, J. Phys. Appl. Phys. 40 (3) (2007) 883, https://doi.org/10.1088/0022-3727/40/3/030.

[32] A. Lucherini, Fundamentals of Thin Intumescent Coatings for the Design of fire-safe Structures, The University of Queensland, Brisbane, 2020. Ph.D., School of Civil Engineering.

[33] N. Gerasimov, Behaviour of Intumescent Coatings Under Non-standard Heating Conditions, The University of Edinburgh, Edinburgh, 2020. Ph.D., School of Engineering.

[34] S. Spyridakis, C. Maluk, A. Orabi, D. Barber, F. Wiesner, Effect of thin intumescent coating type and thickness on the charring of mass timber under varied heat flux exposure, Fire Technol. (2025), https://doi.org/10.1007/s10694-025-01806-x.

[35] M. Yasir, F. Ahmad, P.S.M.M. Yusoff, S. Ullah, M. Jimenez, Latest trends for structural steel protection by using intumescent fire protective coatings: a review, Surf. Eng. 36 (4) (2020) 334–363, https://doi.org/10.1080/02670844.2019.1636536.

[36] J.A. Dreyer, C.E. Weinell, K. Dam-Johansen, S. Kiil, Review of heat exposure equipment and in-situ characterisation techniques for intumescent coatings, Fire Saf. J. 121 (2021) 103264, https://doi.org/10.1016/j.firesaf.2020.103264.

[37] L. Yi, S. Feng, Z. Wang, Y. Ding, Y. Li, Predicting the fire performance of intumescent fire-retardant coating with inert and oxidative reaction schemes, Fire Saf. J. (2025) 104541, https://doi.org/10.1016/j.firesaf.2025.104541.

[38] T. Nazrun, M.K. Hassan, M.R. Hasnat, M.D. Hossain, S. Saha, Improving fire performance of solid aluminium of composite cladding panels incorporating intumescent coatings, Prog. Org. Coating 201 (2025) 109142, https://doi.org/10.1016/j.porgcoat.2025.109142.

[39] M. Bartholmai, R. Schriever, B. Schartel, Influence of external heat flux and coating thickness on the thermal insulation properties of two different intumescent coatings using cone calorimeter and numerical analysis, Fire Mater. 27 (4) (2003) 151–162, https://doi.org/10.1002/fam.823.

[40] F. Zhang, et al., Heat transfer and burning behavior of ADP/MPP epoxy intumescent coatings, J. Loss Prev. Process. Ind. 84 (2023) 105080, https://doi.org/10.1016/j.jlp.2023.105080.

[41] F. Zhang, Y. Sun, Y. Cheng, Study on heat transfer in intumescent fire retardant epoxy coatings during combustion, J. Macromol. Sci. B 56 (8) (2017) 608–622, https://doi.org/10.1080/00222348.2017.1342964.

[42] S. Spyridakis, A. Orabi, C. Maluk, D. Barber, and F. Wiesner, "Charring behaviour of mass timber: a comparison of thin intumescent coatings and plasterboard," Fire Mater., *[Under Review]*.

[43] S. Spyridakis, F. Wiesner, A. Orabi, C. Maluk, Experimental fire studies comparing the charring behaviour of timber protected with thin intumescent coatings and fire rated plasterboard, in: Structures in Fire (Sif 2024), 2024, pp. 1371–1382, https://doi.org/10.30779/cmm_SIF24. Coimbra, Portugal.

[44] A. Hartl, Q.S. Razzaque, A. Lucherini, C. Maluk, Comparative study on the fire behaviour of fire-rated gypsum plasterboards vs. thin intumescent coatings used in mass timber structures. https://doi.org/10.14264/4040b08, 2020.

[45] A. Lucherini, J.P. Hidalgo, J.L. Torero, C. Maluk, Influence of heating conditions and initial thickness on the effectiveness of thin intumescent coatings, Fire Saf. J. 120 (2021) 103078, https://doi.org/10.1016/j.firesaf.2020.103078.

[46] A. Lucherini, Q.S. Razzaque, C. Maluk, Exploring the fire behaviour of thin intumescent coatings used on timber, Fire Saf. J. 109 (2019) 102887, https://doi.org/10.1016/j.firesaf.2019.102887.

[47] S. Spyridakis, J. Carrascal, F. Wiesner, D. Barber, C. Maluk, Exploring the influence of heating conditions in the charring profile of bare timber and timber protected with a thin intumescent coating, in: *World Conference on Timber Engineering (WCTE 2023)*, Oslo, Norway, 2023, pp. 1644–1652, https://doi.org/10.52202/069179-0221.

[48] S. Spyridakis, A. Orabi, W. Wu, C. Maluk, D. Barber, F. Wiesner, Impact of opaque and transparent thin intumescent coatings on the heat release rate of mass timber, in: World Conference on Timber Engineering (WCTE 2025), 2025, pp. 4815–4824, https://doi.org/10.52202/080513-0592. Brisbane, Australia.

[49] M. Jimenez, S. Duquesne, S. Bourbigot, Intumescent fire protective coating: toward a better understanding of their mechanism of action, Thermochim. Acta 449 (1-2) (2006) 16–26, https://doi.org/10.1016/j.tca.2006.07.008.

[50] M. Wagner, Thermal Analysis in Practice: Fundamental Aspects, Carl Hanser Verlag, 2018.

[51] Y. Zhu, F. Zhang, L. Xing, W. Xie, Y. Cheng, Construction and verification of a heat transfer model for intumescent coatings, Prog. Org. Coating 167 (2022) 106868, https://doi.org/10.1016/j.porgcoat.2022.106868.

[52] C. Maluk, L. Bisby, M. Krajcovic, J.L. Torero, A heat-transfer rate inducing system (H-TRIS) test method, Fire Saf. J. 105 (2019) 307–319, https://doi.org/10.1016/j.firesaf.2016.05.001.

[53] O. Zybina, M. Gravit, Intumescent Coatings for Fire Protection of Building Structures and Materials, Springer, 2020.

[54] R. Ross, Wood handbook — wood as an engineering material, in: General Technical Report FPL-GTR-282, U.S. Department of Agriculture, Forest Service, Forest Products Laboratory, 2021.

[55] R. Boone, E. Wengert, Guide for using the oven-dry method for determining the moisture content of wood, in: Forestry Facts, University of Wisconsin, 1998.

[56] J.V. Beck, Thermocouple temperature disturbances in low conductivity materials, ASME J. Heat Mass Transf. (1962) 124–131, https://doi.org/10.1115/1.3684310.

[57] I. Pope, J.P. Hidalgo, R.M. Hadden, J.L. Torero, A simplified correction method for thermocouple disturbance errors in solids, Int. J. Therm. Sci. 172 (2022) 107324, https://doi.org/10.1016/j.ijthermalsci.2021.107324.

[58] S. Bourbigot, M. Le Bras, S. Duquesne, M. Rochery, Recent advances for intumescent polymers, Macromol. Mater. Eng. 289 (6) (2004) 499–511, https://doi.org/10.1002/mame.200400007.
[59] B. Schartel, T.R. Hull, Development of fire-retarded materials—interpretation of cone calorimeter data, Fire Mater. 31 (5) (2007) 327–354, https://doi.org/10.1002/fam.949.
[60] R.D. Peacock, P.A. Reneke, R.W. Bukowski, V. Babrauskas, Defining flashover for fire hazard calculations, Fire Saf. J. 32 (4) (1999) 331–345, https://doi.org/10.1016/S0379-7112(98)00048-4.
[61] D. Drysdale, An Introduction to Fire Dynamics, John Wiley & Sons, 2011.
[62] M.J. Hurley, et al., SFPE Handbook of Fire Protection Engineering, fifth ed., Springer, New York, 2016.
[63] R.H. White, M. Dietenberger, Wood products: thermal degradation and fire. Encyclopedia of Materials: Science and Technology, Elsevier Science Ltd., 2001, pp. 9712–9716.
[64] A.I. Bartlett, R.M. Hadden, L.A. Bisby, A review of factors affecting the burning behaviour of wood for application to tall timber construction, Fire Technol. 55 (2019) 1–49, https://doi.org/10.1007/s10694-018-0787-y.
[65] J. König, L. Walleij, *Timber Frame Assemblies Exposed to Standard and Parametric Fires. Part 2: a Design Model for Standard Fire Exposure* (Rapport/Trätek, 2000. ISSN 1102-1071 ; 1001).
[66] L. Shi, M.Y. Chew, A review of thermal properties of timber and char at elevated temperatures, Indoor Built Environ. (2021), https://doi.org/10.1177/1420326X211035557, 1420326X211035557.